



Turkington, G., Gamage, K. A.A. and Graham, J. (2018) Beta detection of strontium-90 and the potential for direct in situ beta detection for nuclear decommissioning applications. *Nuclear Instruments and Methods in Physics Research. Section A: Accelerators, Spectrometers, Detectors, and Associated Equipment*, 911, pp. 55-65. (doi:[10.1016/j.nima.2018.09.101](https://doi.org/10.1016/j.nima.2018.09.101))

There may be differences between this version and the published version. You are advised to consult the publisher's version if you wish to cite from it.

<http://eprints.gla.ac.uk/171859/>

Deposited on 24 October 2018

Enlighten – Research publications by members of the University of
Glasgow

<http://eprints.gla.ac.uk>

Beta detection of strontium-90 and the potential for direct in situ beta detection for nuclear decommissioning applications

Graeme Turkington^{a,1,*}, Kelum A.A. Gamage^{a,1}, James Graham^{b,1}

^a*Electronics & Electrical Engineering, James Watt South Building, School of Engineering, University of Glasgow, Glasgow, United Kingdom, G12 8QQ*

^b*National Nuclear Laboratory, Sellafield, Seascale, United Kingdom, CA20 1PG*

Abstract

Strontium-90 is one of the primary beta-emitting radionuclides found at nuclear decommissioning sites. Monitoring its activity in the environment is of utmost importance given its radiotoxicity. Current procedures for the beta detection of strontium-90 are time consuming, produce secondary waste and expensive. There is a demand for real-time in situ radiostrontium monitoring in groundwater at nuclear decommissioning sites. This paper presents a review of existing techniques for strontium-90 monitoring and examines a novel approach through direct beta detection with a gallium arsenide photodiode based detector. A proof of concept detector was modelled in the physics simulation software, Geant4, and evaluated as candidate for in situ detection of beta emitting radionuclides. The simulation results indicate that the detector is physically capable of counting 89.86% of incident 0.546 MeV electrons from a 1 mm range in water. This validation will provide the basis for further development of an in situ beta detector.

Keywords: strontium, beta, radiation, detection, photodiode, gallium-arsenide, groundwater

*Corresponding author

Email addresses: g.turkington.1@research.gla.ac.uk (Graeme Turkington), kelum.gamage@glasgow.ac.uk (Kelum A.A. Gamage), james.graham@nnl.co.uk (James Graham)

¹The authors declare no conflict of interest.

²All colour images should be black and white for print

1. Introduction

Strontium-90, ^{90}Sr , is a beta emitting radioisotope produced during nuclear fission and has been dispersed into the environment as a result of accidents at nuclear power plants, leaks from nuclear waste storage and as fallout from nuclear weapons testing. Commonly known as a "bone seeker", ^{90}Sr is chemically similar to fellow alkaline metal calcium, and when it is ingested into the body it has the propensity to accumulate in bone structure [1, 2]. Given the long half-life of ^{90}Sr , 28.8 years [3], its presence in the body can lead to prolonged irradiation of skeletal bone structure, increasing the risk of damage to bone marrow, leukaemia and other bone cancers [4, 5]. As a consequence, it is of great importance to monitor its activity in the environment, particularly in groundwater surrounding nuclear facilities.

^{90}Sr is one of the major beta emitting radionuclides found at the Sellafield site in Cumbria, UK. Leaks and spills from corroded Magnox fuel cladding silos and neutralised nitrate containing wastes [4, 6] have introduced radiostrontium into the environment, where it has mixed with groundwater. Currently, counting beta emitting radionuclides is a long and arduous process. Samples must be collected from groundwater boreholes, transported to a laboratory, and processed with hazardous chemicals before the activity can be measured. With nuclear decommissioning set to continue at sites like Sellafield for the next 100 years and more, these procedures present logistical and financial challenges for the nuclear industry. The recent disaster at the Fukushima Daiichi nuclear power plant (FDNPP) has brought increased scrutiny on the proliferation of ^{90}Sr in the environment and highlighted the need for rapid and agile measurement procedures [7, 8].

Traditionally, contaminated groundwater is collected for analysis from monitoring boreholes installed into the groundwater table. Within an aquifer comprised of unconsolidated deposits, a filter pack and slotted PVC screen are typically installed into a borehole at a target depth. These features prevent the influx of aquifer material while allowing water to flow into the borehole. Water samples may then be pumped to the surface and transported to the laboratory where ^{90}Sr activity is determined by radiochemical analysis. This paper presents a review of the current techniques used in beta detection and explores the potential for in situ beta-counting by direct detection with gallium arsenide photodiode based detectors. This scenario is illustrated in Figure 1, where a detector is placed directly into contaminated groundwater in the screened interval of a borehole.

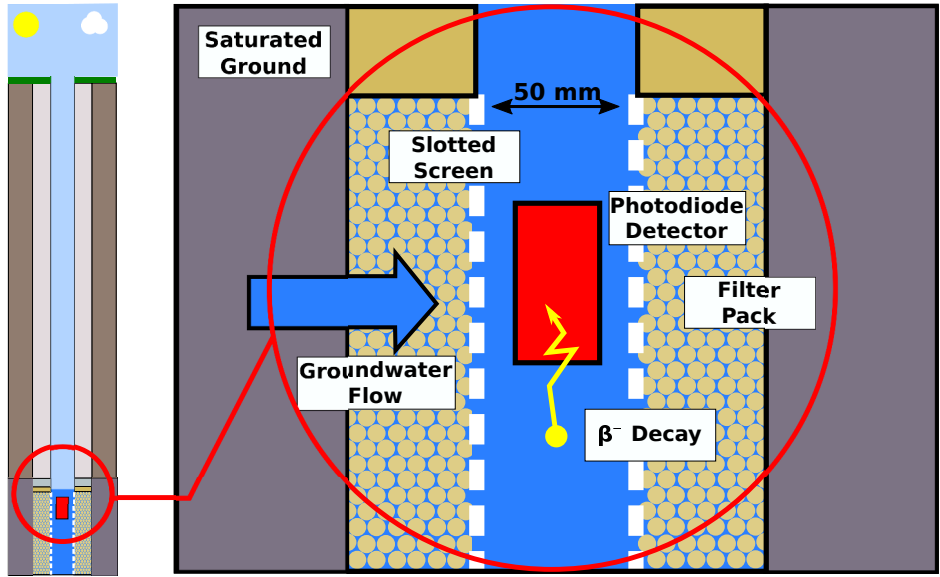
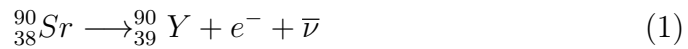


Figure 1: A simplified diagram of a typical groundwater borehole scenario, and the prospective deployment of an in situ photodiode detector.

38 2. Beta radiation

39 Beta particles are electrons (e^-) or positrons (e^+) which are emitted dur-
 40 ing nuclear decay processes. When an unstable nucleus decays via beta
 41 emission, a neutron transforms into a proton and excess energy is shared
 42 between the emitted beta particle (e^-) and an antineutrino ($\bar{\nu}$). Equation 1
 43 illustrates this through the beta-decay of ^{90}Sr . ^{90}Sr is a pure beta-emitter
 44 with a maximum energy of 0.546 MeV [3]. Its daughter nuclei Yttrium-90,
 45 ^{90}Y has a shorter half-life of 64 hours and decays itself, via 2.28 MeV beta
 46 emission, into stable Zirconium-90, ^{90}Zr . The short half-life of ^{90}Y means
 47 that it is often found in secular equilibrium with ^{90}Sr , a property which can
 48 be exploited in radiochemical analysis.



49 Beta particles are emitted over a continuous energy spectrum, from zero
 50 to their maximum end-point energy, see Figure 2. Depending on their initial
 51 energy, beta particles may have a range of a few metres in air, centimetres
 52 in water and millimetres in aluminium [9]. Fast moving electrons typically
 53 ionise matter as a result of inelastic coulomb collisions. When a fast-moving

54 electron is decelerated, usually by the electric field of an atomic nucleus, ex-
 55 cess energy may be released in the form of electromagnetic radiation, known
 56 as Bremsstrahlung radiation [10].

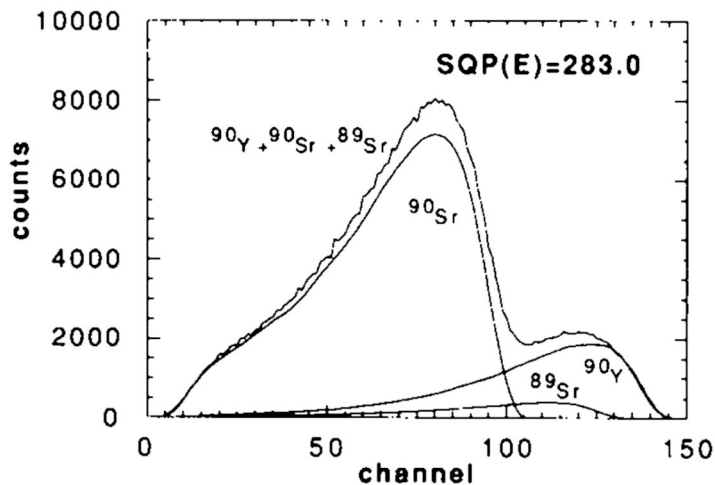


Figure 2: The gross beta spectrum observed, with a liquid scintillation spectrometer, from a sample containing ^{90}Sr , ^{90}Y and ^{89}Sr , where the constituent spectra have been deconvolved. SQP(E) refers to the quenching parameter attributed to the sample [11].

57 As a beta particle travels through matter, coulombic interactions cause
 58 it to lose energy, eventually to the point at which it is no longer detectable.
 59 This limited range in matter has presented difficulties when designing beta
 60 detectors. In an ideal scenario a direct detector would be small, lightweight
 61 and immersible in the detection medium. The detector must operate at very
 62 close range in order to capture particles before they have lost a significant
 63 fraction of their energy. In addition, an ideal device would be compati-
 64 ble with existing borehole dimensions, be low maintenance and produce no
 65 waste. Wireless communications and solar power could remove the need for
 66 obstructive headworks, thereby reducing infrastructure requirements. How-
 67 ever, in the past these technologies have not been sufficiently developed or
 68 readily available. In light of this, many existing techniques have adopted an
 69 indirect approach to detection. Indirect radiation detection sees the source
 70 stimulate a scintillator, which produces flashes of light which are in turn de-
 71 tected by a photomultiplier tube (PMT) or photodiode. These techniques
 72 see water pumped to the surface for sample collection, necessitating surface
 73 infrastructure and regular maintenance.

74 3. Existing Methods for ^{90}Sr monitoring

75 When a sample of unknown radionuclear composition is collected from
76 the environment, the overlapping of their energy spectra makes it difficult
77 to identify individual beta emitters by spectroscopy. For many beta moni-
78 toring techniques, it is essential to isolate the target radionuclide from the
79 sample matrix, thereby removing any other source of radiation entering the
80 detector. There are a number of different methods which can be employed to
81 achieve this, including precipitation [12], liquid-liquid extraction [13], solid-
82 phase extraction [14] and chromatography [15]. When multiple radionuclides
83 are present in the sample, which is inevitable as ^{90}Sr decays to ^{90}Y , it is
84 possible to resolve radionuclides by their spectra provided their beta energies
85 differ significantly [16]. This is achieved by measuring activity over multiple
86 energy windows, and using the resulting information to mathematically re-
87 solve the individual energy spectra of the radionuclides present. C.K. Kim
88 et al. demonstrated a variation on this technique designed for rapid response
89 to emergency scenarios. Their two window approach generated results with
90 minimum detectable limits compliant with IAEA safety standards, with a
91 counting time of just 1.5 hours [17].

92 Once a radionuclide has been isolated, it can be measured using existing
93 beta counting devices, such as gas ionisation chambers and liquid scintilla-
94 tion counters (LSC). Gas ionisation counting is one of the oldest radiation
95 counting techniques, and measures the avalanche of charge induced as ionis-
96 ing radiation traverses a gas. Despite no longer being at the cutting edge of
97 technology, proportional gas counters have remained popular over the years
98 due to their simplicity, cheap construction and low operational costs. They
99 are still used in the standard procedure for ^{90}Sr monitoring in seawater by
100 the Japanese Government [18]. Liquid scintillation counting (LSC) sees a
101 cocktail of organic fluorescence compounds stimulated by ionising radiation
102 into the emission of light which can be detected and used to determine the
103 activity of a radioactive source. Given the low energy of some beta-emitters
104 and the relatively short penetration depth, LSC has become the most widely
105 used technique for measuring pure beta emitters [19]. However, beta count-
106 ing by Cherenkov radiation and gas proportional counters are the primary
107 groundwater counting procedure used at Sellafield. Provided the composi-
108 tion of the groundwater sample is known, gross beta counting may offer a
109 cheaper and quicker alternative. However, naturally occurring ^{40}K and ^{90}Sr
110 may conceal ^{90}Sr contamination from nuclear waste, meaning results are not

111 suitable. This section shall review the Cherenkov counting procedure, from
112 sample preparation to activity counting, and highlight the short-comings of
113 this technique for nuclear decommissioning applications.

114 *3.1. Groundwater sample collection and pre-treatment*

115 In a traditional groundwater monitoring programme, samples of ground-
116 water are obtained from installed monitoring boreholes, typically through
117 either a dedicated or portable pump [20]. Samples for gross beta analysis are
118 then filtered, if a dissolved concentration measurement is required, before
119 collection in a pre-acidified plastic container [21], which gives a maximum
120 recommended holding time of 1 month or 2 months for ^{90}Sr .

121 *3.2. Radiochemical separation*

122 Many beta counting procedures cannot resolve the spectra of different
123 beta emitting particles, therefore in order to accurately determine the activity
124 of ^{90}Sr in an environmental groundwater sample, it must be separated from
125 contaminants and other radionuclides which may interfere with the counting
126 process. A number of techniques have been developed over the years, each
127 with its own advantages and disadvantages. This section shall investigate the
128 three most commonly used procedures, precipitation, liquid-liquid extraction
129 and extraction chromatography.

130 The oldest method for radiostrontium separation is by precipitation. In
131 this procedure, strontium is separated from calcium by exploiting the dif-
132 ferent solubilities of Ca and Sr nitrates in concentrated fuming nitric acid
133 [22, 12]. Radium, lead and barium are collected with barium chromate and
134 the remaining fission products are eliminated with iron hydroxide. ^{90}Y can be
135 separated with hydroxide precipitation and prepared as an oxalate, ready for
136 counting [12]. This procedure, and ones similar to it, have been developed,
137 popularised and standardised since the 1960s. The precipitation technique
138 was popularised because it is robust, efficient and can be applied to large
139 volumes of samples. However it is also laborious, precipitations must be re-
140 peated several times to sufficiently extract strontium from the sample [23, 24].
141 In addition, the health and safety risks, posed through the use of extremely
142 hazardous chemicals, has motivated the development of more rapid and safe
143 techniques.

144 The liquid-liquid extraction technique selectively isolates radionuclides
145 with the use of two immiscible chemical solvents, typically water and an
146 organic solvent. When the analyte is favourably soluble in the solvent, it

147 will distribute itself from one phase to another, almost completely [13]. This
 148 concept can be used to either separate ^{90}Y from the sample, for indirect
 149 measurement of ^{90}Sr activity, or for selective extraction of ^{90}Sr using crown
 150 ethers. ^{90}Y stripping from the sample is achieved with the use of tri-n-
 151 butyl phosphate (TBP), an organic extractant compound [25]. The organic
 152 solvent must then be discarded by washing the sample with water, leaving the
 153 remaining ^{90}Y to be precipitated to oxalate form and counted by Cherenkov
 154 methods.

155 Extraction chromatography with crown ethers was investigated by Horowitz
 156 et. al. in 1990. A crown ether, 4,4,(5')-bis(tert-butyl cyclohexano)-18-crown-
 157 6 in 1-octanol, was sorbed onto an inert substrate and used to selectively
 158 capture the strontium ions of interest [15]. Given the simplicity of prepa-
 159 ration of the ether, and its strong performance in removing strontium from
 160 a nitric acid sample, the ether was commercialised and is now sold as Sr
 161 Resin, produced by EiChrom Industries, Inc [24]. Sr Resin has been widely
 162 adopted in the nuclear industry because it is simple, can be completed in a
 163 few hours and is attractive economically since the resin can be reused. How-
 164 ever, as the properties of Sr Resin were further investigated, some downsides
 165 were revealed. The process of acidifying large volumes of water samples re-
 166 quires precipitation which is time-consuming and may be completed at the
 167 expense of some strontium [26], particularly relevant when considering low
 168 activity samples. Other extraction chromatography products have been man-
 169 ufactured, including 3M EmporeTM Strontium Rad Disks and AnaLig®(R)
 170 gels. EmporeTM Rad Disks consist of a mesh of PTFE (teflon) fibres hosting
 171 AnaLig Sr-01TM selective adsorption chromatographic ligands [14, 27]. Es-
 172 sentially these filters consist of specifically crafted polymers, templated on
 173 the desired molecule for extraction. The result is a very selective procedure
 174 which is capable of separation ^{90}Sr from even its daughter nuclei, ^{90}Y [28].

Table 1: A comparison of radiochemical separation procedures for ^{90}Sr in groundwater.

Method	Avg. radiochemical yield ^{85}Sr %	Avg. Activity $\pm 2\text{U}$ (Bq dm ⁻³)
3M Empore TM Sr Rad Disk	96	377.6 \pm 43.2
AnaLig® Sr-01(60–100 mesh)	99	328.8 \pm 36.9
AnaLig® Sr-01(230–425 mesh)	97	383.9 \pm 43.3
Sr®(R) Resin	89	319.8 \pm 34.4
Liquid extraction —TBP	86	377.9 \pm 25.0
Carbonate precipitation	54	375.5 \pm 45.5

175 A comparative investigation of five different radiochemical separation

176 techniques for ^{90}Sr in water was undertaken by J. Ometakova et al. in a 2011
177 study [29]. The traditional techniques of strontium separation, carbonate
178 co-precipitation and TBP liquid-liquid extraction, were compared along side
179 commercial Solid Phase Extraction (SPE) techniques using 3M EmporeTM
180 Strontium Rad Disks and AnaLig(R) Sr-01 resin at two different mesh levels.
181 The results, summarised in table 1, compare modern SPE extraction with
182 older techniques. SPE achieved higher radiochemical yields while also being
183 substantially quicker and easier to complete compared to liquid-liquid ex-
184 traction and precipitation. Separation using 3M EmporeTM Strontium Rad
185 Disks was possible in 20 minutes. The authors also found that the tradi-
186 tional methods incurred large volumes of liquid waste as well as the use of
187 hazardous concentrated acids. This is of significance to the nuclear decom-
188 missioning industry where thousands of samples must be prepared each year,
189 it is highly desirable to reduce the production of secondary waste as much
190 as possible.

191 3.3. Cherenkov radiation counting

192 When a charged particle moves through a medium with a velocity greater
193 than the phase velocity of light in that medium, energy is released in the
194 form of light known as Cherenkov radiation. Typically the photons released
195 as Cherenkov radiation are from the UV and visible portion of the electro-
196 magnetic spectrum, hence the characteristic blue glow which can be observed
197 in images from the interior of nuclear reactors. This phenomenon has been
198 utilised in the detection of beta particles released from ^{90}Sr and its daughter
199 nuclei. To produce Cherenkov radiation in a medium, such as water, beta-
200 particles must exceed a threshold energy which is dependent on the refractive
201 index of the medium [30, 31]. As such, the refractive index of the selected
202 medium can be used to discriminate between different sources of radiation as
203 the maximum energy of emitted energy from the radioisotope must greatly
204 surpass the threshold energy, given the spectrum of energised beta-particles
205 released [32]. The light produced by Cherenkov radiation can be measured
206 with existing commercial liquid scintillators [33, 34, 35].

207 Cherenkov radiation counting has a few advantages over similar liquid
208 scintillation techniques. The sample used in Cherenkov counting does not
209 need to be incorporated into a scintillation cocktail, resulting in more ef-
210 ficient sample preparation, disposal and the ability to reuse samples [34].
211 One of the primary performance limiting factors in Cherenkov counting is
212 known as quenching. This is any process which reduces the intensity of

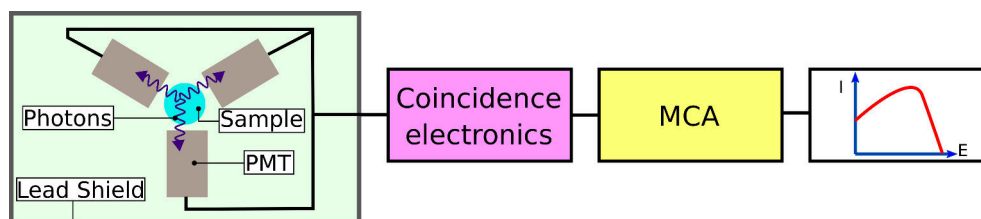


Figure 3: A schematic view of the primary components in a typical TDCR LSC device.

213 light available for detection by the PMTs. The primary quenching effect in
 214 Cherenkov counting is colour quenching, simply a consequence of discoloura-
 215 tion of the sample, which contributes to the absorption of light emitted dur-
 216 ing the Cherenkov process. However, this can be compensated by calibration
 217 with a colour quench correction curve [35, 36].

218 An alternative is to use the Triple to Double Coincidence Ratio (TDCR)
 219 technique. TDCR has recently become popular with many national metrol-
 220 ogy institutes as a method of determining primary activity standards. It is
 221 an absolute method of determining radioactivity in a source and requires no
 222 reference to internal or external sources. TDCR requires a liquid scintilla-
 223 tion detector with three photomultiplier tubes (PMT) uniformly arranged
 224 around a sample, Figure 3, with an electronics package capable of recording
 225 triple and double coincidence events [37]. The activity of the source is calcu-
 226 lated with a free-parameter statistical model, which considers assumptions
 227 about the number of electrons generated during a decay event in the detector
 228 [38, 39].

229 J. M. Olfert et. al. investigated a method for the rapid determination of
 230 ^{90}Sr and ^{90}Y in water samples by liquid scintillation and Cherenkov counting
 231 [40]. Groundwater samples were collected from the discharge of a ground-
 232 water plume, filtered and acidified in preparation for counting. This study
 233 compared five different techniques for ^{90}Sr analysis: direct TDCR counting of
 234 ^{90}Y , LS counting for ^{90}Sr and ^{90}Y after radiochemical separation, Cherenkov
 235 counting for ^{90}Y after radiochemical separation and LS counting of the ^{90}Sr
 236 sample for ^{90}Y in growth. After direct Cherenkov counting of ^{90}Y , the sam-
 237 ples were radiochemically separated, using Sr and DGA-N resins, into ^{90}Sr
 238 and ^{90}Y . The ^{90}Sr sample was counted via LSC, and recounted after 8 days
 239 to allow for ^{90}Y in growth. Meanwhile, the ^{90}Y sample was measured by
 240 Cherenkov and LSC. Each sample was counted with a Hidex 300SL TDCR
 241 Liquid Scintillation counter [41]. The results produced by each technique

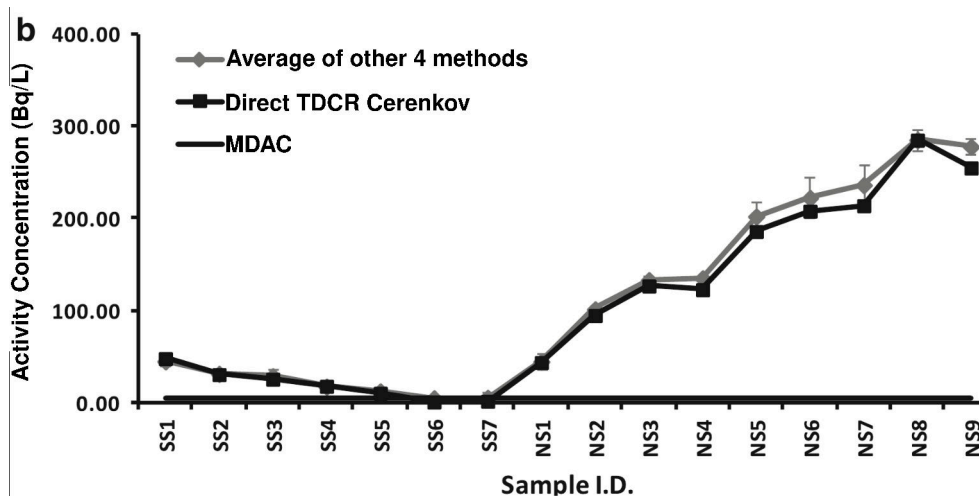


Figure 4: A comparison of radiochemical separation procedures for ^{90}Sr in groundwater [40]. MDAC refers to the minimum detectable activity concentration.

242 were consistent with each other, validating the TDCR technique against the
 243 standard radiochemical procedure as a method for detecting beta-emitting
 244 radionuclides (see Fig. 3). This affirmation highlights TDCR as a technique
 245 with a number of advantages over radiochemical separation. The procedure
 246 is fast, requires no sample preparation and does not suffer from chemical
 247 quenching. However, radiochemical separation assures that no interfering
 248 radionuclides are present in the sample and results were produced within 1
 249 day.

250 Initially, with a lack of suitable detectors commercially available, many
 251 TDCR systems were purpose-built in laboratories. In the last few years,
 252 commercially produced detectors have become available such as the Hidex
 253 300SL. However, these detectors are large and immobile, rendering them ill-
 254 suited for in situ detection purposes. The European Metrology Research
 255 Programme (EMRP) and the Joint Research Project MetroFission launched
 256 an initiative to design and develop a portable TDCR device for use in situ at
 257 next generation power plants. Four different national metrology institutes,
 258 NPL (UK), ENEA (Italy), LNHB (France), and PTB (Germany) were tasked
 259 with producing a device. Each design had to be distinct yet conform with
 260 a number of fundamental design principles. Chiefly that the device must fit
 261 into a standard car and be light enough to be comfortably handled by one
 262 person [42].

263 The PTB design featured three channel photomultipliers packed into a
264 compact optical chamber itself ensconced in a foam carrying case, a portable
265 mini NIM bin to house the electronics and a portable PC for data acqui-
266 sition and processing [37, 43]. Initial validations of the device found that
267 it could measure the activity of some high energy nuclides, such as ^{90}Sr ,
268 with uncertainties under 1% and a similar percentage deviation from refer-
269 ence TDCR measurements. However, the performance of the device suffered
270 when measuring lower energy emitters as uncertainty contributions from low
271 count statistics and background radiation took on increased significance in
272 the model. It was concluded that while the device was not of the standard
273 required for metrology applications, the device could be sufficient for other
274 field-based research. Indeed each of the devices produced in the design ini-
275 tiative showed promising results in their initial validation measurements and
276 offer promising potential for further development.

277 Many procedures for Cherenkov counting of ^{90}Sr have been developed
278 over the years [44, 45] and the technique has become the primary method for
279 ^{90}Sr analysis at the Sellafield decommissioning site. Currently, groundwater
280 samples are pumped from boreholes and transported to laboratories for anal-
281 ysis. Strontium is separated using ion exchange resins, and counted in a two
282 window approach[46]. The activity of the ^{90}Sr source is counted immediately
283 after separation and again, after 20 to 30 days, once it has achieved secular
284 equilibrium with its daughter nuclei ^{90}Y . The activity of the original ^{90}Sr
285 source is determined by the ingrowth of ^{90}Y . Across the Nuclear Decomis-
286 sioning Authority, thousands of groundwater and solid samples require anal-
287 ysis each year, and there is demand for ever more data to provide a greater
288 understanding of groundwater systems [46]. As this demand increases, the
289 financial and temporal costs associated with Cherenkov counting will mount.
290 This puts financial and organisational strain on decommissioning sites and
291 is the motivation for an alternative approach.

292 *3.4. Demand for next generation beta detectors*

293 Sellafield, and other nuclear decommissioning sites, must plan their oper-
294 ation for the next 100+ years and there is an increasing demand for data to
295 be collected more frequently and in real-time while decreasing lifetime mon-
296 itoring costs. This functionality will allow sites to immediately respond to
297 unexpected spikes in groundwater mobility, which may have gone undetected
298 with existing monitoring routines. In addition, more frequent data acquisi-
299 tion would allow decommissioning sites to enhance their understanding of

300 groundwater systems and the daily factors which influence contaminant mo-
301 bility. This would provide evidence in the development of conceptual models
302 for radionuclide transport in groundwater, and enhance safety assessments
303 which indicate whether groundwater strontium is being managed correctly.
304 Although more rapid and streamlined versions of existing techniques have
305 been developed [18, 28] , these are reserved for use in emergency scenarios
306 and still suffer from the same drawbacks in terms of chemical waste, sample
307 collection and expenses.

308 Beta detection by gas ionisation chambers, liquid scintillation counting
309 and Cherenkov counting is very sensitive and precise, with minimum de-
310 tectable limits of activity well below the standards required to meet World
311 Health Organisation (WHO) guidelines, 10 BqL^{-1} [47]. Indeed, LSC has
312 been adopted by many metrology institutions across the world, such is the
313 calibre of results it can provide. However, the practicalities of these proce-
314 dures present hazards for workers through manual handling of samples and
315 the risk of exposure to radiation. Samples must be collected from remote
316 locations, delivered to laboratories, treated with chemicals, counted and fi-
317 nally disposed of. As these procedures must be completed hundreds of times
318 per year for the duration of the facility’s lifetime, there will be significant
319 operating costs and production of secondary wastes.

320 This paper seeks to propose an alternative approach to beta spectroscopy,
321 through direct in situ detection of beta radiation. Attempts have been made
322 to produce in situ versions of the weighty lab-based detectors required for
323 existing techniques, but this does little to satisfactorily address the demands
324 for real-time radiostrontium monitoring in groundwater. This paper con-
325 siders a novel approach where the detector is deployed within groundwater
326 boreholes, directly at the source of radiation. This would require a radia-
327 tion detector that is sensitive to beta radiation, offers real-time detection,
328 while also being highly portable. Such a device would be unburdened by
329 time-consuming sample collection and chemical treatment procedures. One
330 potential solution comes in the form of photodiodes, adapted for use as direct
331 radiation detectors. Photodiodes are devices designed to convert light into
332 electrical current, recognisably used in solar panels. The same mechanisms
333 that allow for the conversion of visible light to current also apply to ionising
334 radiation.

335 4. PIN photodiodes

336 This research aims to develop a highly mobile, fast and efficient beta-
337 radiation detector, free from the lengthy chemical separation and counting
338 procedures outlined in the previous section. To this end, PIN photodiodes
339 are being investigated as candidate for a light weight radiation detector.
340 Initially developed to detect photons and used as an alternative to PMTs,
341 photodiodes have been increasingly investigated in recent years as a tool
342 for direct radiation detection. In comparison with gas-filled or scintillation
343 detectors, semiconductors have a lower energy requirement for charged par-
344 ticle detection resulting in superior energy resolution [48]. They now have a
345 number of applications in medical imaging, dosimetry, power generation and
346 high-energy radiation experiments[49, 50, 51, 52].

347 In contrast to PN-junction semiconductors, PIN photodiodes have a large
348 intrinsic layer separating the p and n-type layers. Figure 5 illustrates a
349 simplified configuration of a PIN photodiode and its interaction with ionising
350 radiation. As radiation enters the intrinsic layer, it disrupts electron-hole
351 pairs which are swept up by a reverse-biased voltage and the resulting current
352 is measured. The more energy is deposited, the greater the current pulse
353 produced. By extending the size of the depleted region, a larger volume is
354 presented for ionising radiation to fully deposit its energy within the sensitive
355 region of the detector.

356 A number of materials are used to construct semiconductor photodiodes,
357 each with their own strengths and weaknesses. Silicon and germanium
358 rapidly emerged as widely used semiconductors, largely due to early advances
359 in manufacturing allowing for high quality devices to be made cheaply and
360 quickly. However, these materials have properties which make them less
361 than ideal candidates for in situ beta detection. Germanium detectors offer
362 excellent energy resolution but, due to a very narrow bandgap of 0.66 eV,
363 require cooling to liquid nitrogen temperatures to reduce thermally induced
364 noise [10]. This clearly makes germanium ill-suited for mobile applications.
365 While silicon has a wider bandgap, 1.1 eV, it still requires cooling and its low
366 atomic number, 14, means it has relatively poor stopping power for ionising
367 radiation.

368 4.1. Gallium arsenide

369 Gallium arsenide has a number of properties which make it an attrac-
370 tive alternative to silicon and other semiconductor materials. Gallium and

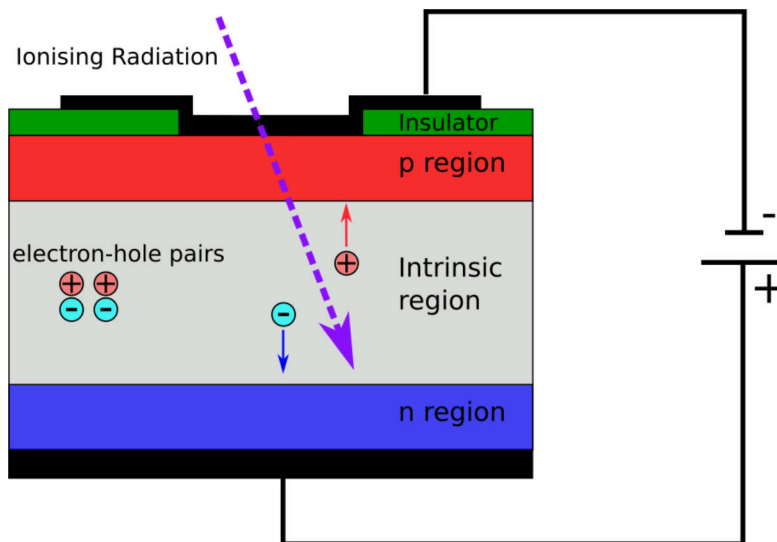


Figure 5: A simplified view of ionising radiation generating a current pulse in a PIN photodiode operating under reverse biased voltage.

371 arsenic have atomic numbers of 31 and 33, respectively, resulting in the ma-
 372 terial having greater stopping power for ionising radiation, like X-rays, in
 373 comparison with silicon devices [53, 54]. The bandgap of the compound
 374 material, 1.42 eV, is wide enough that devices can be operated at room tem-
 375 perature [55, 53, 54] without overwhelming thermal noise. Table 2 compares
 376 some of the fundamental properties of GaAs and Si. As the electron mobility
 377 of the GaAs is approximately 6 times greater than Si, this should allow for
 378 a device which functions over a shorter time scale.

Table 2: A comparison between the semiconductor properties of Si and GaAs [56].

Property	Silicon	Gallium-arsenide
z	14	32
ρ (gcm^{-3})	2.33	5.31
Radiation Length (cm)	9.36	2.3
Pair Production Energy (eV)	3.55	4.27
Electron Mobility (cm^2/Vs)	1500	7000-8500

379 Radiation detectors, unsurprisingly, are bombarded with ionising radia-
 380 tion and it is important that the device is not degraded or significantly dam-
 381 aged over time. The ability of a material to withstand the damage is known

382 as its radiation hardness. There are two principle ways in which radiation can
 383 negatively affect a semiconductor, displacement damage and ionisation dam-
 384 age. Displacement damage refers to the permanent physical dislocation of
 385 atoms from their lattice positions by incoming radiation. This produces de-
 386 fects in the material resulting in intermediate energy states, facilitating easier
 387 separation of electron-hole pairs, thus generating current and contributing to
 388 noise in the detector. Additionally, charges can become trapped on intermedi-
 389 ate levels, which will negatively affect counting statistics. Ionisation damage
 390 occurs after energy deposition in the detector frees electron-hole pairs which
 391 drift to other locations and become trapped. When sufficient concentrations
 392 of charge are trapped, localised parasitic electric fields can develop [57].

393 A. Sagatova et al investigated the radiation hardness of GaAs devices
 394 against gamma radiation, high energy electrons and fast neutrons [58]. The
 395 detectors, beams and doses used in their experimentation is summarised in
 396 Table 3. An Am²⁴¹ gamma spectrum was captured at each dosage and the
 397 results of electron damage on the spectra acquired, photopeak area, charge
 398 collection efficiency (CCE) and full width half maximum (FWHM), indicative
 399 of the energy resolution, were documented. Curiously, the results reported
 400 indicated that low doses, 1 kGy, of electron damage may even improve the
 401 performance of the detector, and this was attributed to the radiation damage
 402 compensating for pre-existing defects in the device. The study found that
 403 the damaging induced by electrons was up to 10 times worse than that of
 404 gamma photons, and up to 1000 time worse for neutrons. Indeed, the device
 405 was no longer functional after a dose of 0.576 kGy of fast neutrons, and was
 406 still functional, albeit in a limited capacity, after the full course of electrons
 407 and gamma.

Table 3: Experiments carried out by A. Sagatova et al [58] determining the radiation hardness of GaAs.

Radiation	Detector Thickness (μm)	Energy (MeV)	Max Dose (kGy)
Gamma	250	1.33	1140
Electrons	230	5	104
Neutrons	300	2-30	3.215

408 The radiation damage in GaAs sensors has been investigated by numerous
 409 studies [56, 59, 60] and has been compared favourably with silicon [60]. The
 410 strong radiation hardness of GaAs, has seen the material used radiation
 411 harsh environments like high energy particle accelerators and satellites, and

412 suggests that GaAs is a viable candidate for use at nuclear waste disposal
413 facilities.

414 In recent years, GaAs photodiodes garnered increasing interest for their
415 potential as X-ray imaging devices. One of the hurdles in this has developing
416 detectors with intrinsic layers thick enough to stop energetic radiation such
417 as X-rays, with as few defects as possible to maintain strong energy resolu-
418 tion. Detectors designed for beta detection will likely require similarly thick
419 intrinsic layers.

420 The major imperfection associated with GaAs crystals is known as the
421 EL2 defect. This defect is present in many fabrications techniques, including
422 Metal Organic Chemical Vapour Deposition (MOCVD) and Liquid Encap-
423 sulated Czochralski (LEC), however is notably absent in Molecular Beam
424 Epitaxy (MBE) [61]. The exact nature of this defect is the subject of much
425 debate, but it is known to produce a midgap deep level, essentially a trap
426 for electrons. The presence of the EL2 defect restricts the sensitive volume
427 of the device, which is crucial for radiation detection. The ionised form of
428 the defect meanwhile reduces electron lifetime, dampening charge collection
429 efficiency and therefore energy resolution [51]. This defect has presented a
430 stumbling block in the use of GaAs photodiodes in sensitive applications,
431 such as medical imaging and radiation detection.

432 *4.2. Applications in radiation detection*

433 One of the limiting factors in the adoption of GaAs devices as radiation
434 detectors has been the presence of defects, such as EL2, in the bulk material.
435 This induces a small sensitive layer thickness, low values of electron charge
436 collection efficiency, current oscillations in the detector and non-uniform field
437 distribution. A. V. Tyazhev et al [62] noted these flaws in the LEC process.
438 As an alternative, they proposed using chromium compensated GaAs layers.
439 Their study validated the composition through I-V characterisation, electric
440 field distribution tests and CCE assessment. It was found that chromium
441 doped GaAs offers high resistivity, thickness approaching 1 mm, more uni-
442 form electric field distribution and functional levels of CCE for use in X-ray
443 pixel detectors. Figure 6 offers a point of comparison between a LEC GaAs
444 device, operating at 250 V, and a chromium compensated device, on the
445 right. The function plotted is $F = 1 - T$, where T is the spatial distribution
446 of light transmission through the detector thickness. This demonstrates that
447 chromium compensated GaAs structures offer a more uniform electric field

448 distribution, which is stable over a range of operating voltages. This unifor-
 449 mity of electric field is significant, because it allows for detectors with very
 450 thick intrinsic layers to be operational.

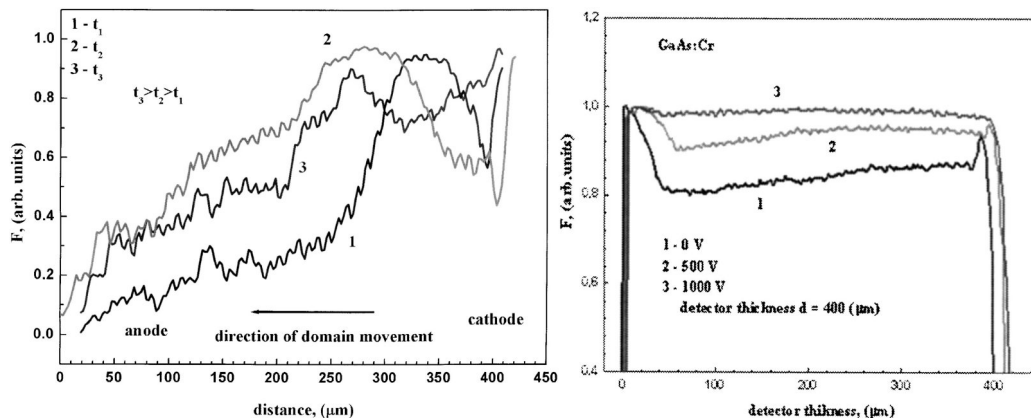


Figure 6: These graphs plot the function F , a cypher for electric field distribution, through a LEC fabricated detector, left, and a chromium compensated detector, right [62].

451 Building on A. V. Tyazhev's research, M.C. Veale et al [51] produced 500
 452 μm thick chromium compensated GaAs devices and tested their potential for
 453 X-ray and γ -ray spectroscopy and imaging. The GaAs wafer was affixed to
 454 Schottky electrodes, etched with an 80×80 array of $200 \mu\text{m}$ anode pixels and
 455 bonded to a HEXITEC ASIC readout chip. I-V characteristics for the device
 456 were measured at 280 K and 298 K, with the room temperature resistivity
 457 measured as $2.5 \times 10^9 \Omega\text{cm}$. To investigate the spectroscopic ability of the
 458 detector, an ^{241}Am γ spectrum was collected at 280 K. The FWHM of the
 459 60 keV photopeak in this figure is 2.9 keV. As a proof of concept for X-ray
 460 imaging a test object, fitted with different materials, and imaged by 5-80 keV
 461 X-rays. This is illustrated in Figure 7. The materials, from clockwise, are
 462 adhesive putty, indium, lead, tin, and indium. The image produced, right,
 463 indicates the ability of the detector to distinguish between different materials
 464 thereby functioning as an imaging device.

465 Elsewhere, C. Erd et al [63] developed a spectroscopic X-ray imaging de-
 466 vice based on epitaxially grown GaAs. The prototype array was fabricated
 467 by growing a $325 \mu\text{m}$ epitaxial intrinsic GaAs layer onto a $200 \mu\text{m}$ n+ sub-
 468 strate, topped with a $6 \mu\text{m}$ p+ layer, completing the PIN structure. The 1.1
 469 cm^2 surface area was etched into a grid of 32×32 pixels. Optimal operating
 470 conditions for the reverse bias, 60 V, were established and the energy resolu-

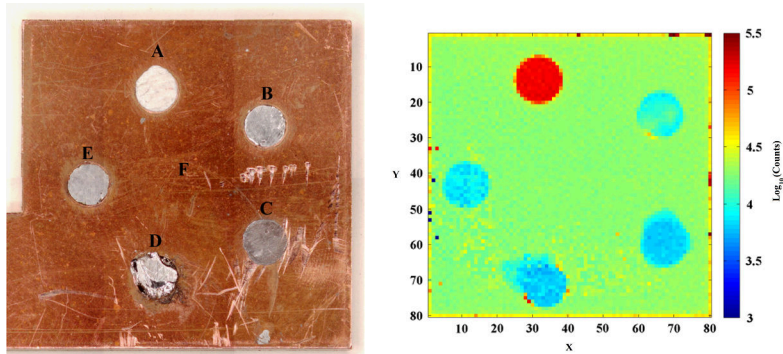


Figure 7: A proof of concept demonstration of X-ray imaging with a GaAs sensor [51].

471 tion of individual pixels were found to range from approximately 290 eV for
 472 a 5.9 keV beam and 780 eV for a 100 keV beam. These results were obtained
 473 at room temperature, and the investigations into variation of resolution with
 474 temperature found a 10% gain in resolution as the device was cooled to 5 °C
 475 with negligible improvements at cooler temperatures.

476 The results found here can be contrasted with the previously cited study
 477 into chromium compensated GaAs. C. Erd et al's device was anticipated to
 478 achieve a resolution of 0.5 keV for the 60 keV photopeak on an ^{241}Am source
 479 at room temperature. The same photopeak has a resolution of 2.9 keV for
 480 the GaAs:Cr detector. The GaAs:Cr detector has a thicker intrinsic layer,
 481 which should contribute to better energy resolution in principle, however
 482 this device was not based on epitaxially grown GaAs, as was the case with
 483 C. Erd's device. Veale et al selected the LEC growth technique in order to
 484 grow a thick material bulk whereas the MBE technique allows for the precise
 485 and orderly growth of crystal layers, at lower temperatures than LEC, reduc-
 486 ing the risk of defect inducing effects like interdiffusion [64]. Deficiencies in
 487 material quality can give rise to charge collection inefficiencies which intro-
 488 duce noise to the detriment of energy resolution. Furthermore, C. Erd et al
 489 developed and tested low noise pre-amplifier designs which may have played
 490 an additional role in the superior energy resolution of their device. C. Erd,
 491 et al also found the FWHM of a 5.9 keV photopeak, 0.26 keV, which can be
 492 contrasted with a more recent study by G. Lioliou et al [54]. They conducted
 493 a comprehensive characterisation of MOVCD GaAs photodiodes, fabricating
 494 200 μm and 400 μm diameter device with 10 μm thick intrinsic layers. The
 495 detectors have energy resolutions of 0.69 keV and 0.73 keV respectively. The

496 authors suggest their relatively thin device suffers primarily from the effects
497 dielectric noise in addition to white series noise and Fano noise. These fac-
498 tors are all correlated with the capacitance of the device, which is reduced in
499 thicker devices. This can give rise to a number of benefits including increased
500 quantum efficiency and lower pulse shaping times [10]. Future work will see
501 the authors reconsider the design of the pre-amplifier by combining the pho-
502 todiode and the junction gate field-effect transistor (JFET) into the same
503 substrate with the aim of reducing dielectric noise. Additionally, further re-
504 finements in device passivation may reduce surface leakage current and bring
505 the energy resolution performance closer to the previously discussed devices.

506 There are many other studies investigating the burgeoning field of X-ray
507 spectroscopy by GaAs photodiodes and it can be concluded that these devices
508 have potential in this field [65, 66]. These studies have validated some of the
509 advantages of using GaAs including radiation hardness, energy resolution
510 and room temperature operation. In addition to giving insight into suitable
511 fabrication techniques, I-V characteristics and potential readout electronics.
512 However, there have been few documentations of their application to beta
513 radiation.

514 Barnett, Lees, and Bassford attempted direct detection of ^3H and ^{14}C
515 beta particles with GaAs photodiodes [67]. Their detectors were grown by
516 MBE and photolithographically etched into 200 μm diameter diodes with 2
517 μm thick intrinsic layers. Beta propagation through the device was simulated
518 with the Monte Carlo software, CASINO [68]. Particles ranging in energy
519 from 1 keV to 156.48 keV were simulated, investigating their penetration
520 depth and deposition of energy within the detector. Figure 8 shows the
521 results of the simulation of 156.48 keV electrons. It can be observed that
522 the thin intrinsic layer of this detector is not sufficient to stop incoming
523 radiation of this energy, and the electrons penetrate into the substrate layer
524 of the diode. This indicates that a much thicker intrinsic layer would be
525 required for beta particles approaching the energy of those released by ^{90}Sr
526 and ^{90}Y . Other results from this study indicate that the limiting factor on
527 the detection of low energy beta particles, less than 5 keV, is the p-type layer
528 on the surface of the detector. This region attenuates the particles sufficiently
529 such that the maximum proportion of their energy deposited in the intrinsic
530 layer is only 50%. The detector was used to capture ^3H and ^{14}C spectra
531 which, after calibration, showed accordance with accepted spectra for these
532 nuclides. The results presented here are promising for the potential of GaAs
533 detectors, although evidently the intrinsic layer is likely much too thin for

534 efficient ^{90}Sr detection.

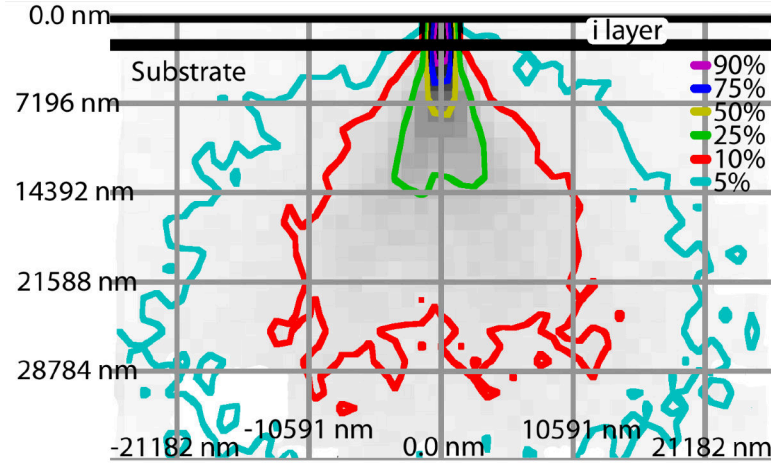


Figure 8: The percentage of initial energy, 156.48 keV, of beta particles deposited in a GaAs detector [67]

535 Lioliou and Barnett [69] characterised GaAs p^+i-n^+ mesa photodiodes to
536 assess their potential as low energy beta spectrometers with a view to using
537 them in applications for space plasma physics. GaAs photodiodes were fab-
538 ricated for this study at the EPSRC National Centre for III-V Technologies,
539 Sheffield, with a $10\ \mu\text{m}$ undoped GaAs intrinsic layer sandwiched between a
540 $0.50\ \mu\text{m}$ thick GaAs p^+ layer and a $1\ \mu\text{m}$ n^+ layer. Reportedly the thickest
541 X-ray mesa photodiodes produced to date, the wafers used for beta spec-
542 troscopy had a $200\ \mu\text{m}$ diameter. Initially, the detectors were simulated with
543 the Monte Carlo simulation software, CASINO. A point source of 4,000 elec-
544 trons, varying from 1 keV to 66 keV, were fired at the detector surface and
545 the depth of their penetration is summarised in Figure 9. Simulations were
546 run with and without the presence of the Ohmic contact required on the
547 detector, which covered 45% of the detector's surface. The simulation pre-
548 dicted a maximum external quantum efficiency of 49% from a 66 keV source,
549 with the major limiting factors being the absorption of electrons in the top
550 layers of the diode and the Ohmic contacts.

551 Following on from the simulation, a real-world validation was carried out.
552 A ^{63}Ni source was placed 5 mm above the surface of the GaAs photodiode,
553 which was operating under a 10 V reverse bias. After a counting time of
554 400 s the collected beta spectrum was compared with the accepted spectrum

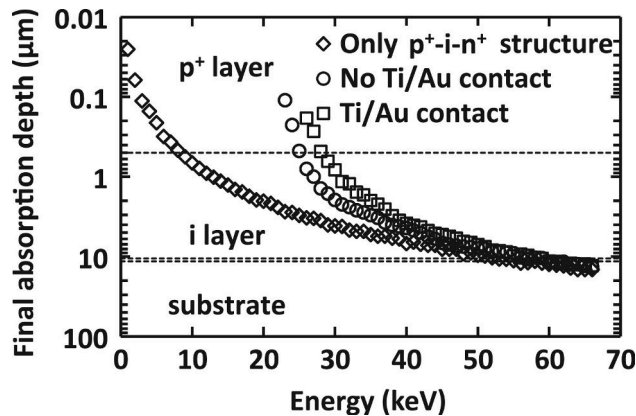


Figure 9: The simulated absorption depth of electrons in a GaAs p^+i-n^+ detector as a function of their energy [55]

555 of a ^{63}Ni beta source, normalised to reflect experimental conditions. The
 556 maximum energy observed in the intrinsic region was approximately 50 keV,
 557 suggesting that maximum energy particles were losing 16 keV. This was a 9
 558 keV difference from the maximum energy predicted in the simulation. This
 559 discrepancy was attributed to the absorption of energy in insensitive sections
 560 of the detector, including the p^+ layer in the device, the nickel protective layer
 561 around the source and the air gap between source and detector. While these
 562 results were promising for the potential of GaAs photodiodes as electron
 563 spectrometers, they were conducted with a device designed for X-ray rather
 564 than beta-spectrometry in mind. The response of the device to much higher
 565 energy electrons remains to be seen, whether they are stopped by the intrinsic
 566 layer in sufficient numbers to produce a clear signal. It is likely that detection
 567 of ^{90}Sr with GaAs photodiodes will require devices thicker than the 10 μm
 568 devices which have been tested in these studies. The photodiodes fabricated
 569 for X-ray detection have demonstrated that it is possible to produce thicker
 570 detectors and by producing a chromium doped or epitaxially grown device
 571 can address the defects which have previously hindered the development of
 572 GaAs devices.

573 5. Monte-Carlo simulations

574 Reviewing the literature has highlighted some tentative studies applying
 575 GaAs photodiodes as beta radiation detectors, however, these have only been
 576 applied to low energy beta emitters. The devices used have relatively thin

577 intrinsic layers, particularly in comparison with some of the detectors being
 578 developed for X-ray detection. A proof of concept simulation was developed
 579 to investigate the potential for GaAs as a beta detector in a groundwa-
 580 ter borehole scenario, for energies on the scale of ^{90}Sr and ^{90}Y decay. The
 581 physics simulation package, Geant4, was used to construct a basic model of
 582 a GaAs detector and simulate its interaction with beta-particles. Geant4 is a
 583 Monte Carlo simulation based software and is written in the object-oriented
 584 programming language C++ [70]. Step by step the software tracks the path
 585 of radiation as it travels through matter. At each step the probability of
 586 interaction and random number generation predict the next step along the
 587 particle's track. The exact nature of the physics processes invoked in the
 588 simulation and their cross-sections are defined by the "Physics List" selected
 589 for the simulation. Geant4 includes a number of reference Physics Lists and
 590 this simulation used the FTFP_BERT list, the Geant4 default which is valid
 591 for electrons up to 100 TeV.

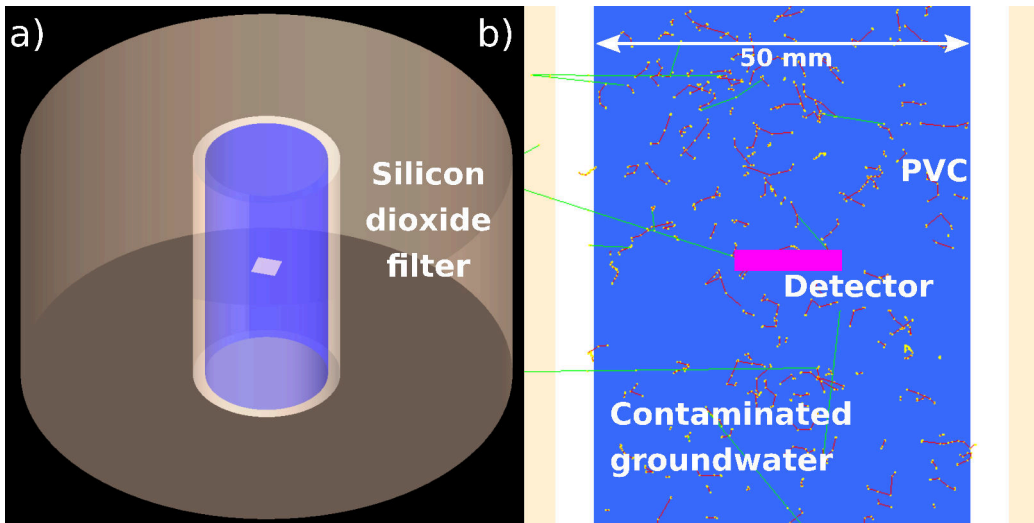


Figure 10: An overall visualisation of the Geant4 simulation can be seen in image a). Image b) is a cross section of the well, filled with ^{90}Sr contaminated groundwater. As nuclei decay beta particles are released and traverse the water in erratic paths. They are either fully absorbed, deflected, or release bremsstrahlung radiation, the long straight lines. Bright dots mark steps in the particle's path.

592 The proof of concept detector was based on a device created by C. Erd
 593 et al [63]. This design was selected due to the relatively thick intrinsic layer,
 594 especially in comparison with previous detectors applied to beta radiation.

595 Matching the thickness of the intrinsic layer, 0.325 mm, and surface area, 1.1
 596 cm², a GaAs detector was created in Geant4 code and placed in a modelled
 597 groundwater borehole. Figure 10a visualises the borehole with the detector
 598 submerged in groundwater. A cross section of the scenario is seen in Figure
 599 10b. Here, decaying ⁹⁰Sr particles are randomly dispersed throughout the
 600 groundwater. As ⁹⁰Sr decays, electrons, the short erratic trajectories, are re-
 601 leased and tracked as they travel through space. Bright dots mark steps along
 602 the particle's trajectory before it is fully absorbed by the environment or the
 603 detector. As the particles interact the detector they are either backscattered,
 604 pass through the detector while only depositing a fraction of their energy, or
 605 fully absorbed within the intrinsic layer of the detector. Their energy and
 606 path are recorded, along with the number of counts in the detector for the
 607 entire run. The long and straight particle lines shown in this image represent
 608 photons, likely the result of the Bremsstrahlung effect. The anti-neutrinos
 609 released during beta decay are hidden for visual clarity.

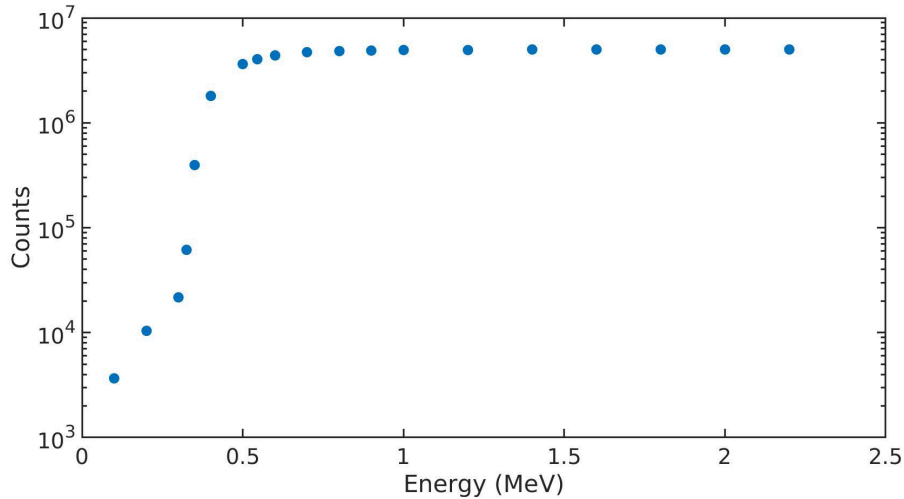


Figure 11: The number of counts recorded in the detector for increasing beams of electron energy. Errors range from ± 35 to $\pm 1.290 \times 10^3$ and as such are not clearly visible on the graph.

610 The initial simulation examined whether the detector had sufficient stop-
 611 ping power to detect electrons emitted during ⁹⁰Sr and ⁹⁰Y decay. A particle
 612 gun was positioned 0.1 mm from the surface of the detector and the energy
 613 of the beam was increased from 0.1 MeV to 2.2 MeV. Each run consisted of

614 5×10^6 electrons and the results can be seen in Figure 11. Fewer counts are
615 observed at lower energies, attributed to the increased likelihood of low en-
616 ergy electrons be absorbed before detection and to backscatter on the surface
617 of the detector. As the energy increases to 1.2 MeV, nearly the entire run of
618 electrons, 99% on average, deposit energy in the detector and are counted.
619 However, this does not account for how much energy is being deposited by
620 each particle. Some electrons are backscattered, leaving only a fraction of
621 their energy, or simply pass through the detector. When designing the pho-
622 todiodode, it will be of utmost importance to ensure the intrinsic layer is thick
623 enough to fully capture the energy of particles released by the radionuclides
624 of interest, thereby being capable of fully recording their beta spectra.

625 The second simulation investigated how the intensity of the radiation
626 detected varied with increasing distance from the source. A 0.546 MeV beam
627 of electrons was fired at the detector from 0.1 cm away increasing to 8.5 cm.
628 Figure 12 displays the results. The number of counts observed by the detector
629 decays exponentially with increasing distance. Particles released within few
630 millimetres from the detector's surface, dropping to tens of counts at a range
631 of 8 cm. This detector aims to be used in situ, and will have to operate at
632 some distance from the source, so the detectable range of the detector is a
633 key characterisation.

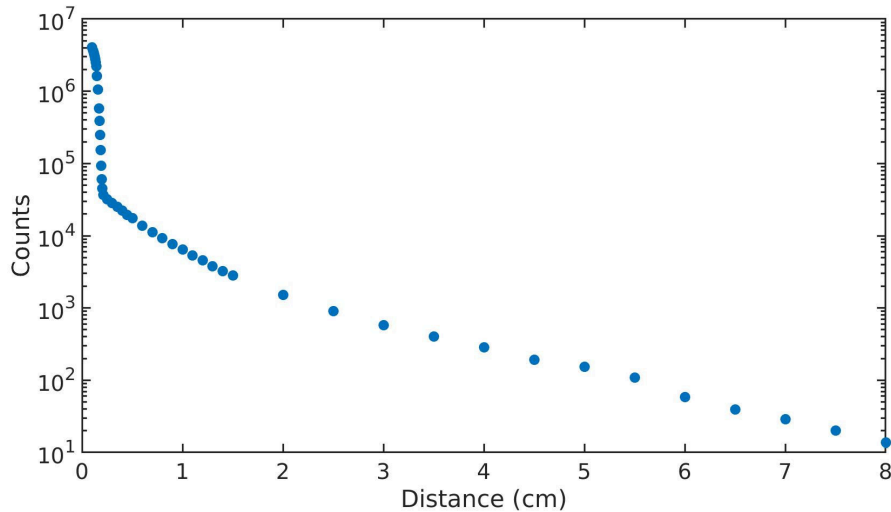


Figure 12: The number of counts detected as the detector is moved further away from a 0.546 MeV electron beam source.

634 As an exhibition of the potential application of the detector, the device
 635 was used to collect a spectrum of radiation from a contaminated groundwater
 636 source. A 5 cm deep cylinder of water was randomly filled with decaying ^{90}Sr
 637 particles. A full decay chain was realised for each ^{90}Sr particle, resulting in
 638 ^{90}Y production and decay to stable Zr. The simulation ran for 1×10^7 decay
 639 events. The spectrum of beta radiation captured in the detector is seen
 640 in Figure 13. The first peak is largely comprised of beta particles released
 641 during ^{90}Sr decay, and the lower second peak is indicative of ^{90}Y decay, which
 642 tails off at a much higher energy, approximately 1.8 MeV. It should be noted
 643 that the particles generated during this simulation must travel some distance
 644 before reaching the detector, and as such will have already lost some of their
 645 kinetic energy to the surrounding environment.

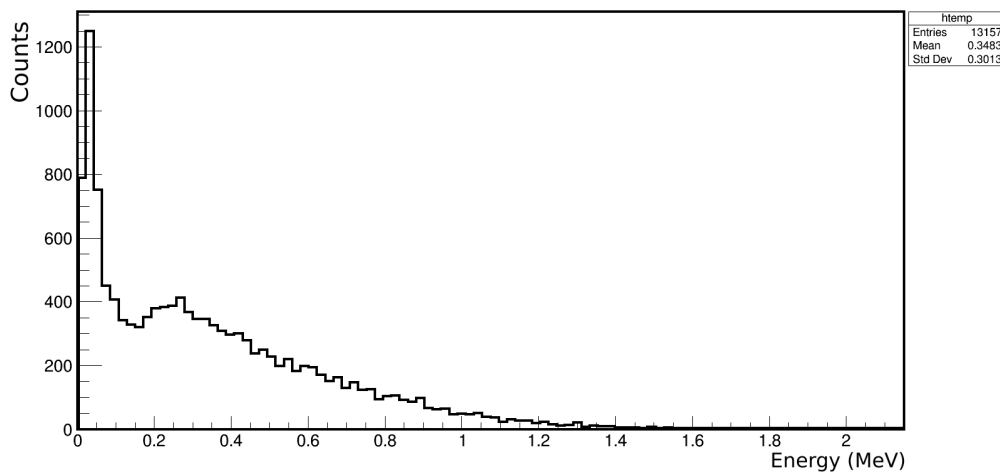


Figure 13: The spectra of beta particle energy recorded in the detector after 1×10^7 ^{90}Sr decay events were simulated.

646 The simulation results presented here are encouraging for the potential
 647 of GaAs photodiodes as in situ detectors for the radiometric assay of ^{90}Sr .
 648 It has been demonstrated that a detector of real-world proportions can be
 649 successfully detect beta particles of the energy scale required in a situation
 650 modelled on a real world scenario. This suggests there is potential to use
 651 GaAs photodiodes in the development of an in situ beta detector.

652 **6. Conclusions**

653 This paper has presented a review of existing methods for the radiometric
654 analysis of ^{90}Sr in the environment and their suitability, or lack thereof, for
655 in situ detection has been examined. Nuclear decommissioning sites have
656 a demand for real-time, in situ, monitoring of radionuclides in groundwater
657 to improve their response to fluctuations in groundwater activity and to
658 further evaluate waste management. Current techniques are lab-based, time
659 consuming and expensive. While there have been attempts to reduce the
660 time-scales involved in these procedures, and create more mobile detectors,
661 these only go part way to addressing the practical difficulties associated with
662 these techniques. A novel approach based on the direct detection of beta
663 radiation has been proposed. GaAs photodiodes were examined for their
664 ability to directly detect ionising radiation, and their suitability for beta
665 radiation was validated through simulation.

666 The research presented here has suggested that GaAs is indeed a strong
667 candidate for an in situ beta detector. The wide bandgap of the material
668 means it can eschew the cooling requirements of other semiconductors, re-
669 ducing the size and weight of the detector. Meanwhile its radiation hardness
670 suggests GaAs devices are well suited for operation at sites of nuclear waste
671 and spillage. Development of such a device will enable real-time counting
672 of beta radiation in difficult to reach areas, such as groundwater boreholes,
673 reducing risk of exposure to workers.

674 Initial Geant4 simulations have demonstrated that GaAs has right phys-
675 ical properties to detect beta radiation. The fabrication technique selected
676 can have an influence on the defects present in the device and its operating
677 characteristics, energy resolution and efficiency. Photodiode junction layers
678 and electronics readout systems will also influence the energy deposition of
679 radiation in the detector.

680 **7. Acknowledgements**

681 The authors would like to acknowledge the Nuclear Decommissioning
682 Authority and the University of Glasgow for funding support.

683 **References**

- 684 [1] A. Panahifar, D. M. L. Cooper, M. R. Doschak, 3-D localization of
685 non-radioactive strontium in osteoarthritic bone: Role in the dynamic

- 686 labeling of bone pathological changes, *Journal of Orthopaedic Research*
687 33 (11) (2015) 1655–1662. doi:10.1002/jor.22937.
- 688 [2] M. Zamburlini, A. Pejović-Milić, D. R. Chettle, C. E. Webber, J. Gy-
689 orffy, In vivo study of an x-ray fluorescence system to detect bone stron-
690 tium non-invasively, *Physics in Medicine & Biology* 52 (8) (2007) 2107.
691 doi:10.1088/0031-9155/52/8/005.
- 692 [3] V. Chiste, Table de Radionucleides, [http://www.lnhb.fr/nuclides/Sr-](http://www.lnhb.fr/nuclides/Sr-90_tables.pdf)
693 [90_tables.pdf](http://www.lnhb.fr/nuclides/Sr-90_tables.pdf) (May 2005).
- 694 [4] S. H. Wallace, S. Shaw, K. Morris, J. S. Small, A. J. Fuller, I. T.
695 Burke, Effect of groundwater pH and ionic strength on strontium sorp-
696 tion in aquifer sediments: Implications for ^{90}Sr mobility at contam-
697 inated nuclear sites, *Applied Geochemistry* 27 (8) (2012) 1482–1491.
698 doi:10.1016/j.apgeochem.2012.04.007.
- 699 [5] H. Tazoe, H. Obata, T. Yamagata, Z. Karube, H. Nagai, M. Yamada,
700 Determination of strontium-90 from direct separation of yttrium-90 by
701 solid phase extraction using DGA Resin for seawater monitoring, *Ta-*
702 *lanta* 152 (2016) 219–227. doi:10.1016/j.talanta.2016.01.065.
- 703 [6] J. Small, S. Wallace, I. Burke, Strontium-90 mobility in contaminated
704 nuclear facilities and groundwater, *NNL Science* 1 (2) (2014) 26.
- 705 [7] N. Kavasi, S. Sahoo, A. Sorimachi, S. Tokonami, T. Aono, S. Yoshida,
706 Measurement of Sr-90 in soil samples affected by the Fukushima Daiichi
707 Nuclear Power Plant accident, *Journal of Radioanalytical and Nuclear*
708 *Chemistry* 303 (3) (2015) 2565–2570. doi:10.1007/s10967-014-3649-1.
- 709 [8] S. K. Sahoo, N. Kavasi, A. Sorimachi, H. Arae, S. Tokonami, J. W.
710 Mietelski, E. Łokas, S. Yoshida, Strontium-90 activity concentration in
711 soil samples from the exclusion zone of the Fukushima daiichi nuclear
712 power plant, *Scientific Reports* 6 (2016) 23925. doi:10.1038/srep23925.
- 713 [9] L. Pages, E. Bertel, H. Joffre, L. Sklavenitis, Energy loss, range, and
714 bremsstrahlung yield for 10-keV to 100-MeV electrons in various ele-
715 ments and chemical compounds, *Atomic Data and Nuclear Data Tables*
716 4 (Journal Article) (1972) 1–27. doi:10.1016/S0092-640X(72)80002-0.

- 717 [10] G. F. Knoll, Radiation Detection and Measurement, 3rd Edition, Wiley,
718 New York, 2000.
- 719 [11] A. Grau Malonda, L. Rodriguez Barquero, A. Grau Carles, Radioactiv-
720 ity determination of ^{90}Y , ^{90}Sr and ^{89}Sr mixtures by spectral deconvol-
721 ution, Nuclear Instruments and Methods in Physics Research Section
722 A: Accelerators, Spectrometers, Detectors and Associated Equipment
723 339 (1-2) (1994) 31–37. doi:10.1016/0168-9002(94)91774-4.
- 724 [12] N. A. Chieco, The Procedures Manual of the Environmental Measure-
725 ments Laboratory, U.S. Department of Energy I (28) (1997) 524.
- 726 [13] A. N. Anthemidis, K.-I. G. Ioannou, Recent developments in ho-
727 mogeneous and dispersive liquid–liquid extraction for inorganic el-
728 ements determination. A review, Talanta 80 (2) (2009) 413–421.
729 doi:10.1016/j.talanta.2009.09.005.
- 730 [14] D. M. Beals, W. G. Britt, J. P. Bibler, D. A. Brooks, Radionuclide anal-
731 ysis using solid phase extraction disks, Journal of Radioanalytical and
732 Nuclear Chemistry 236 (1-2) (1998) 187–191. doi:10.1007/BF02386340.
- 733 [15] E. P. Horwitz, M. L. Dietz, D. E. Fisher, Separation and preconcen-
734 tration of strontium from biological, environmental, and nuclear waste
735 samples by extraction chromatography using a crown ether, Analytical
736 Chemistry 63 (5) (1991) 522–525. doi:10.1021/ac00005a027.
- 737 [16] M. F. L’Annunziata, M. J. Kessler, Chapter 7 - Liquid Scintillation Anal-
738 ysis: Principles and Practice, in: M. F. L’Annunziata (Ed.), Handbook
739 of Radioactivity Analysis (Third Edition), Academic Press, Amsterdam,
740 2012, pp. 423–573. doi:10.1016/B978-0-12-384873-4.00007-4.
- 741 [17] C. K. Kim, A. Al-Hamwi, A. Törvényi, G. Kis-Benedek, U. San-
742 sone, Validation of rapid methods for the determination of radiostron-
743 tium in milk, Applied Radiation and Isotopes 67 (5) (2009) 786–793.
744 doi:10.1016/j.apradiso.2009.01.036.
- 745 [18] M. Uesugi, R. Watanabe, H. Sakai, A. Yokoyama, Rapid method
746 for determination of ^{90}Sr in seawater by liquid scintillation count-
747 ing with an extractive scintillator, Talanta 178 (2018) 339–347.
748 doi:10.1016/j.talanta.2017.09.041.

- 749 [19] Ryszard Broda and Philippe Cassette and Karsten Kossert, Radionu-
750 clide metrology using liquid scintillation counting, *Metrologia* 44 (4)
751 (2007) S36.
- 752 [20] ISO 5667-11:2009, Water quality – Sampling – Part 11: Guidance on
753 sampling of groundwaters, Tech. rep., International Organization for
754 Standardization (2009).
- 755 [21] ISO 5667-3:2012, Water quality – Sampling - Part 3: Preservation and
756 handling of water samples, Tech. rep., BSI Standards Institution (2012).
- 757 [22] N. Vajda, C.-K. Kim, Determination of radiostrontium isotopes: A re-
758 view of analytical methodology, *Applied Radiation and Isotopes* 68 (12)
759 (2010) 2306–2326. doi:10.1016/j.apradiso.2010.05.013.
- 760 [23] M. Rodríguez, J. A. Suárez, A. G. Espartero, Separation of radioactive
761 strontium by extraction using chromatographic resin, *Nuclear Instru-
762 ments and Methods in Physics Research Section A: Accelerators, Spec-
763 trometers, Detectors and Associated Equipment* 369 (2) (1996) 348–352.
764 doi:10.1016/S0168-9002(96)80007-6.
- 765 [24] N. Vajda, A. Ghods-Esphahani, E. Cooper, P. R. Danesi, Determi-
766 nation of radiostrontium in soil samples using a crown ether, *Journal
767 of Radioanalytical and Nuclear Chemistry* 162 (2) (1992) 307–323.
768 doi:10.1007/BF02035392.
- 769 [25] T. Jabbar, K. Khan, M. S. Subhani, P. Akhter, Determination of ^{90}Sr
770 in environment of district Swat, Pakistan, *Journal of Radioanalytical
771 and Nuclear Chemistry* 279 (2) (2009) 377–384. doi:10.1007/s10967-
772 007-7277-5.
- 773 [26] J. J. Surman, J. M. Pates, H. Zhang, S. Happel, Development and
774 characterisation of a new Sr selective resin for the rapid determination
775 of ^{90}Sr in environmental water samples, *Talanta* 129 (2014) 623–628.
776 doi:10.1016/j.talanta.2014.06.041.
- 777 [27] S. Dulanska, B. Remenec, L. Matel, D. Galanda, A. Molnar, Pre-
778 concentration and determination of Sr-90 in radioactive wastes using
779 solid phase extraction techniques, *Journal of Radioanalytical and Nu-
780 clear Chemistry* 288 (3) (2011) 705–708. doi:10.1007/s10967-011-1019-9.

- 781 [28] Ž. Grahek, G. Karanović, M. Nodilo, Rapid determination of $^{89,90}\text{Sr}$ in
782 wide range of activity concentration by combination of yttrium, stron-
783 tium separation and Cherenkov counting, *Journal of Radioanalytical*
784 *and Nuclear Chemistry* 292 (2) (2012) 555–569. doi:10.1007/s10967-
785 011-1441-z.
- 786 [29] J. Ometáková, S. Dulanská, L. Mátel, B. Remenec, A comparison of
787 classical ^{90}Sr separation methods with selective separation using molec-
788 ular recognition technology products AnaLig® SR-01 gel, 3M Empore™
789 Strontium Rad Disk and extraction chromatography Sr®Resin, *Jour-
790 nal of Radioanalytical and Nuclear Chemistry* 290 (2) (2011) 319–323.
791 doi:10.1007/s10967-011-1338-x.
- 792 [30] H. H. Ross, Measurement of beta-emitting nuclides using Cerenkov
793 radiation, *Analytical Chemistry* 41 (10) (1969) 1260–1265.
794 doi:10.1021/ac60279a011.
- 795 [31] S. C. Scarpitta, I. M. Fisenne, Cerenkov counting as a complement to liq-
796 uid scintillation counting, *Applied Radiation and Isotopes* 47 (8) (1996)
797 795–800. doi:10.1016/0969-8043(96)00061-9.
- 798 [32] D. Brajnik, S. Korpar, G. Medin, M. Starič, A. Stanovnik, Measurement
799 of ^{90}Sr activity with Cherenkov radiation in a silica aerogel, *Nuclear*
800 *Instruments and Methods in Physics Research Section A: Accelerators,*
801 *Spectrometers, Detectors and Associated Equipment* 353 (1) (1994) 217–
802 221. doi:10.1016/0168-9002(94)91642-X.
- 803 [33] D. D. Rao, S. T. Mehendarge, S. Chandramouli, A. G. Hegde, U. C.
804 Mishra, Application of Cherenkov radiation counting for determination
805 of ^{90}Sr in environmental samples, *Journal of Environmental Radioactiv-
806 ity* 48 (1) (2000) 49–57. doi:10.1016/S0265-931X(99)00053-3.
- 807 [34] I. Cocha, S. Neufuss, Ž. Grahek, M. Němec, M. Nodilo, J. John, The effect
808 of counting conditions on pure beta emitter determination by Cherenkov
809 counting, *Journal of Radioanalytical and Nuclear Chemistry* 310 (2)
810 (2016) 891–903. doi:10.1007/s10967-016-4853-y.
- 811 [35] J. M. Torres, J. F. García, M. Llauradó, G. Rauret, Rapid determination
812 of strontium-90 in environmental samples by single Cerenkov counting

- 813 using two different colour quench curves, *Analyst* 121 (11) (1996) 1737–
814 1742. doi:10.1039/AN9962101737.
- 815 [36] S. Tsroya, O. Pelled, U. German, R. Marco, E. Katorza, Z. Alfassi,
816 Color quench correction for low level Cherenkov counting, 5th Interna-
817 tional Conference on Radionuclide Metrology - Low-Level Radioactiv-
818 ity Measurement Techniques ICRM-LLRMT'08 67 (5) (2009) 805–808.
819 doi:10.1016/j.apradiso.2009.01.038.
- 820 [37] M. Capogni, P. De Felice, A prototype of a portable TDCR sys-
821 tem at ENEA, *Applied Radiation and Isotopes* 93 (2014) 45–51.
822 doi:10.1016/j.apradiso.2014.03.021.
- 823 [38] R. Broda, P. Cassette, K. Kossert, Radionuclide metrology using liquid
824 scintillation counting, *Metrologia* 44 (4) (2007) S36. doi:10.1088/0026-
825 1394/44/4/S06.
- 826 [39] P. Cassette, J. Bouchard, The design of a liquid scintillation counter
827 based on the triple to double coincidence ratio method, *Nuclear Instru-*
828 *ments and Methods in Physics Research Section A: Accelerators, Spec-*
829 *trometers, Detectors and Associated Equipment* 505 (1) (2003) 72–75.
830 doi:10.1016/S0168-9002(03)01023-4.
- 831 [40] J. Olfert, X. Dai, S. Kramer-Tremblay, Rapid determination of Sr-90/Y-
832 90 in water samples by liquid scintillation and Cherenkov counting, *Jour-*
833 *nal of Radioanalytical and Nuclear Chemistry* 300 (1) (2014) 263–267.
834 doi:10.1007/s10967-013-2913-0.
- 835 [41] Hidex 300 SL, <http://hidex.com/products/hidex-300-sl/>.
- 836 [42] P. Cassette, M. Capogni, L. Johansson, K. Kossert, O. Nähle, J. Seph-
837 ton, P. D. Felice, Development of portable Liquid Scintillation coun-
838 ters for on-site primary measurement of radionuclides using the Triple-
839 To-Double Coincidence Ratio method, in: 2013 3rd International
840 Conference on Advancements in Nuclear Instrumentation, Measurement
841 Methods and Their Applications (ANIMMA), 2013, pp. 1–7.
842 doi:10.1109/ANIMMA.2013.6727876.
- 843 [43] O. Nähle, Q. Zhao, C. Wanke, M. Weierganz, K. Kossert, A portable
844 TDCR system, *Applied Radiation and Isotopes* 87 (2014) 249–253.
845 doi:10.1016/j.apradiso.2013.11.084.

- 846 [44] F. Vacap, G. Manjón, M. Garcia-León, Efficiency calibration of a liquid
847 scintillation counter for ^{90}Y cherenkov counting, *Nuclear Instruments*
848 *and Methods in Physics Research Section A: Accelerators, Spectrom-*
849 *eters, Detectors and Associated Equipment* 406 (2) (1998) 267–275.
850 doi:10.1016/S0168-9002(98)91986-6.
- 851 [45] M. Tayeb, X. Dai, E. C. Corcoran, D. G. Kelly, Evaluation of inter-
852 ferences on measurements of $^{90}\text{Sr}/^{90}\text{Y}$ by TDCR Cherenkov counting
853 technique, *Journal of Radioanalytical and Nuclear Chemistry* 300 (1)
854 (2014) 409–414. doi:10.1007/s10967-013-2910-3.
- 855 [46] D. Offin, G. Toon, G. Bolton, Review of Remote Systems for Monitor-
856 ing Radionuclides in Groundwater, *National Nuclear Decommissioning*
857 *Authority NNL 13748* (3) (2016) 55.
- 858 [47] World Health Organization, *Guidelines for Drinking-Water Quality.*,
859 2017, oCLC: 975491910.
- 860 [48] D. S. McGregor, *Semiconductor Counters*, in: C. Grupen, I. Buvat
861 (Eds.), *Handbook of Particle Detection and Imaging*, Springer Berlin
862 Heidelberg, Berlin, Heidelberg, 2012, pp. 377–410. doi:10.1007/978-3-
863 642-13271-1-16.
- 864 [49] S. V. Bulyarskiy, A. V. Lakalin, I. E. Abanin, V. V. Amelichev,
865 V. V. Svetuhin, Optimization of the parameters of power sources
866 excited by β -radiation, *Semiconductors* 51 (1) (2017) 66–72.
867 doi:10.1134/S1063782617010055.
- 868 [50] F. Dubecký, A. Perd’ochová, P. Ščepko, B. Zat’ko, V. Sekerka, V. Nečas,
869 M. Sekáčová, M. Hudec, P. Boháček, J. Huran, Digital X-ray portable
870 scanner based on monolithic semi-insulating GaAs detectors: Gen-
871 eral description and first “quantum” images, *Nuclear Instruments and*
872 *Methods in Physics Research Section A: Accelerators, Spectrom-*
873 *eters, Detectors and Associated Equipment* 546 (1) (2005) 118–124.
874 doi:10.1016/j.nima.2005.03.020.
- 875 [51] M. Veale, S. Bell, D. Duarte, M. French, A. Schneider, P. Seller, M. Wil-
876 son, A. Lozinskaya, V. Novikov, O. Tolbanov, A. Tyazhev, A. Zarubin,
877 Chromium compensated gallium arsenide detectors for X-ray and γ -ray

- 878 spectroscopic imaging, Nuclear Instruments and Methods in Physics Re-
879 search Section A: Accelerators, Spectrometers, Detectors and Associated
880 Equipment 752 (2014) 6–14. doi:10.1016/j.nima.2014.03.033.
- 881 [52] P. H. Gooda, W. B. Gilboy, High resolution alpha spectroscopy with
882 low cost photodiodes, Nuclear Instruments and Methods in Physics Re-
883 search Section A: Accelerators, Spectrometers, Detectors and Associated
884 Equipment 255 (1) (1987) 222–224. doi:10.1016/0168-9002(87)91105-3.
- 885 [53] G. Bertuccio, Prospect for energy resolving X-ray imaging with
886 compound semiconductor pixel detectors, Nuclear Instruments and
887 Methods in Physics Research Section A: Accelerators, Spectrome-
888 ters, Detectors and Associated Equipment 546 (1) (2005) 232–241.
889 doi:10.1016/j.nima.2005.03.015.
- 890 [54] G. Lioliou, M. D. C. Whitaker, A. M. Barnett, High temperature GaAs
891 X-ray detectors, Journal of Applied Physics 122 (24) (2017) 244506.
892 doi:10.1063/1.5005878.
- 893 [55] G. Lioliou, X. Meng, J. S. Ng, A. M. Barnett, Characterization of gal-
894 lium arsenide X-ray mesa p-i-n photodiodes at room temperature, Nu-
895 clear Instruments and Methods in Physics Research Section A: Acceler-
896 ators, Spectrometers, Detectors and Associated Equipment 813 (2016)
897 1–9. doi:10.1016/j.nima.2015.12.030.
- 898 [56] V. B. Chmill, A. V. Chuntunov, A. V. Smol, A. P. Vorobiev, S. S. Khlud-
899 kov, A. A. Koretski, L. S. Okaevitch, A. I. Potapov, V. E. Stepanov,
900 O. P. Tolbanov, K. M. Smith, Particle detector based on GaAs. Radia-
901 tion hardness and spatial resolution, Nuclear Instruments and Methods
902 in Physics Research Section A: Accelerators, Spectrometers, Detectors
903 and Associated Equipment 409 (1) (1998) 247–250. doi:10.1016/S0168-
904 9002(97)01272-2.
- 905 [57] H. Spieler, Oxford University Press, Semiconductor Detector Systems,
906 Vol. 12.;12;, Oxford University Press, Oxford, 2005.
- 907 [58] A. Šagátová, B. Zařko, F. Dubecký, T. Ly Anh, V. Nečas, K. Sedlačková,
908 M. Pavlovič, M. Fülöp, Radiation hardness of GaAs sensors against
909 gamma-rays, neutrons and electrons, Applied Surface Science 395 (2017)
910 66–71. doi:10.1016/j.apsusc.2016.08.167.

- 911 [59] K. Afanaciev, M. Bergholz, P. Bernitt, G. Chelkov, J. Gajewski,
912 M. Gostkin, C. Grah, R. Heller, H. Henschel, A. Ignatenko,
913 Z. Krumshteyn, S. Kulis, W. Lange, W. Lohmann, D. Mokeev,
914 V. Novikov, M. Ohlerich, A. Rosca, A. Saponov, R. Schmidt,
915 S. Schuwalow, O. Tolbanov, A. Tyazhev, Chalmers University of Tech-
916 nology, N. E. Department of Applied Physics, Chalmers tekniska
917 högskola, N. teknik Institutionen för teknisk fysik, Investigation
918 of the radiation hardness of GaAs sensors in an electron beam,
919 JOURNAL OF INSTRUMENTATION 7 (11) (2012) P11022–P11022.
920 doi:10.1088/1748-0221/7/11/P11022.
- 921 [60] V. K. Dixit, S. K. Khamari, S. Manwani, S. Porwal, K. Alexander, T. K.
922 Sharma, S. Kher, S. M. Oak, Effect of high dose γ -ray irradiation on
923 GaAs p-i-n photodetectors, Nuclear Instruments and Methods in Physics
924 Research Section A: Accelerators, Spectrometers, Detectors and Associ-
925 ated Equipment 785 (2015) 93–98. doi:10.1016/j.nima.2015.03.008.
- 926 [61] N. A. Naz, U. S. Qurashi, M. Z. Iqbal, Arsenic antisite defects in
927 p-GaAs grown by metal-organic chemical-vapor deposition and the
928 EL2 defect, Journal of Applied Physics 106 (10) (2009) 103704.
929 doi:10.1063/1.3243162.
- 930 [62] A. V. Tyazhev, D. L. Budnitsky, O. B. Koretskay, V. A. Novikov, L. S.
931 Okaevich, A. I. Potapov, O. P. Tolbanov, A. P. Vorobiev, GaAs radiation
932 imaging detectors with an active layer thickness up to 1mm, Nuclear
933 Instruments and Methods in Physics Research Section A: Accelerators,
934 Spectrometers, Detectors and Associated Equipment 509 (1) (2003) 34–
935 39. doi:10.1016/S0168-9002(03)01545-6.
- 936 [63] C. Erd, A. Owens, G. Brammertz, M. Bavdaz, A. Peacock, V. Lämsä,
937 S. Nenonen, H. Andersson, N. Haack, Hard X-ray test and evalua-
938 tion of a prototype 32×32 pixel gallium–arsenide array, Nuclear Instru-
939 ments and Methods in Physics Research Section A: Accelerators, Spec-
940 trometers, Detectors and Associated Equipment 487 (1) (2002) 78–89.
941 doi:10.1016/S0168-9002(02)00949-X.
- 942 [64] K. Adomi, J. I. Chyi, S. F. Fang, T. C. Shen, S. Strite, H. Morkoç,
943 Molecular beam epitaxial growth of GaAs and other compound semi-
944 conductors, Thin Solid Films 205 (2) (1991) 182–212. doi:10.1016/0040-
945 6090(91)90301-D.

- 946 [65] P. J. Sellin, G. Rossi, M. J. Renzi, A. P. Knights, E. F. Eikenberry,
947 M. W. Tate, S. L. Barna, R. L. Wixted, S. M. Gruner, Performance
948 of semi-insulating gallium arsenide X-ray pixel detectors with current-
949 integrating readout, *Nuclear Instruments and Methods in Physics Re-*
950 *search Section A: Accelerators, Spectrometers, Detectors and Associated*
951 *Equipment* 460 (1) (2001) 207–212. doi:10.1016/S0168-9002(00)01117-7.
- 952 [66] X. Wu, T. Peltola, T. Arsenovich, A. Gädda, J. Härkönen, A. Junkes,
953 A. Karadzhinova, P. Kostamo, H. Lipsanen, P. Luukka, M. Mattila,
954 S. Nenonen, T. Riekkinen, E. Tuominen, A. Winkler, Processing and
955 characterization of epitaxial GaAs radiation detectors, *Nuclear In-*
956 *struments and Methods in Physics Research Section A: Accelerators,*
957 *Spectrometers, Detectors and Associated Equipment* 796 (2015) 51–55.
958 doi:10.1016/j.nima.2015.03.028.
- 959 [67] A. M. Barnett, J. E. Lees, D. J. Bassford, Direct detection of Tritium
960 and Carbon-14 beta particles with GaAs photodiodes, *Journal of Instru-*
961 *mentation* 7 (09) (2012) P09012. doi:10.1088/1748-0221/7/09/P09012.
- 962 [68] Casino, <http://www.gel.usherbrooke.ca/casino/index.html>.
- 963 [69] G. Lioliou, A. M. Barnett, Gallium Arsenide detectors for X-
964 ray and electron (beta particle) spectroscopy, *Nuclear Instruments*
965 *and Methods in Physics Research Section A: Accelerators, Spec-*
966 *trometers, Detectors and Associated Equipment* 836 (2016) 37–45.
967 doi:10.1016/j.nima.2016.08.047.
- 968 [70] Recent developments in Geant4, *Nuclear Instruments and Meth-*
969 *ods in Physics Research Section A: Accelerators, Spectrome-*
970 *ters, Detectors and Associated Equipment* 835 (2016) 186–225.
971 doi:10.1016/j.nima.2016.06.125.